Nanotechnology **21** (2010) 075501 (8pp) doi:10.1088/0957-4484/21/7/075501

Cantilever-based sensing: the origin of surface stress and optimization strategies

Michel Godin[1,7,8], Vincent Tabard-Cossa[2,8], Yoichi Miyahara[3], Tanya Monga[4], P J Williams[5], L Y Beaulieu[6], R Bruce Lennox[4] and Peter Grutter[3]

[1] Department of Physics, University of Ottawa, 150 Louis Pasteur, Ottawa, ON, K1N 6N5, Canada
[2] Stanford Genome Technology Center, Stanford University, 855 California Avenue, Palo Alto, CA 94304, USA
[3] Department of Physics, McGill University, 3600 University Street, Montréal, QC, H3A 2T8, Canada
[4] Department of Chemistry, McGill University, 801 Sherbrooke Street West, Montréal, QC, H3A 2K6, Canada
[5] Department of Physics, Acadia University, PO Box 49 Wolfville, NS, B4P 2R6, Canada
[6] Department of Physics and Physical Oceanography, Memorial University of Newfoundland, St John's, NF, A1B 3X7, Canada

E-mail: mgodin@uottawa.ca

Received 18 October 2009, in final form 17 December 2009
Published 18 January 2010
Online at stacks.iop.org/Nano/21/075501

Abstract
Many interactions drive the adsorption of molecules on surfaces, all of which can result in a measurable change in surface stress. This article compares the contributions of various possible interactions to the overall induced surface stress for cantilever-based sensing applications. The surface stress resulting from adsorption-induced changes in the electronic density of the underlying surface is up to 2–4 orders of magnitude larger than that resulting from intermolecular electrostatic or Lennard-Jones interactions. We reveal that the surface stress associated with the formation of high quality alkanethiol self-assembled monolayers on gold surfaces is independent of the molecular chain length, supporting our theoretical findings. This provides a foundation for the development of new strategies for increasing the sensitivity of cantilever-based sensors for various applications.

S Supplementary data are available from stacks.iop.org/Nano/21/075501/mmedia

1. Introduction

Micromechanical cantilevers show great potential as highly sensitive (bio)chemical sensors. Cantilever-based sensing involves the transduction of a (bio)molecular interaction to a measurable mechanical change in the cantilever resulting from induced surface stresses [1, 2], added mass [3–5] or the transfer of heat [6–9]. In surface stress sensing applications, one side of the cantilever beam is rendered sensitive to a specific target molecule, while the opposing surface is chemically passivated [10]. When target molecules interact with the sensitized surface of the cantilever, the change in surface stress between the sensitized and passivated surfaces results in a measurable mechanical deflection of the cantilever beam. Recently, surface stress sensing has been demonstrated in various clinically important sensing applications (e.g. DNA [11, 12], RNA [13], and protein [14, 15]) and for gas phase detection (e.g. VOCs [16, 17], TNT [18, 19], mercury vapors [20]). Nevertheless, one of the factors that has limited the success of cantilever-based sensing is the relatively low signal-to-noise ratio observed during detection. For instance, biomolecular detection has typically generated small surface stresses ($\sim$0.001–0.01 N m^{-1}). Despite 15 years of cantilever-based sensing research, several start-up companies and the promise of potential applications, this technology has yet

[7] Author to whom any correspondence should be addressed.
[8] These authors contributed equally to this work.

to emerge with a strong presence in the marketplace. If cantilever-based sensing is to become a viable technology in strategic areas such as medical diagnostics, food safety and environmental monitoring, the origins of the surface stress signal need to be better understood and used to significantly improve performance.

Various groups have worked to improve the performance of cantilever-based sensors, typically in one of two ways. Some have modified cantilever geometries and materials in an attempt to increase sensitivity to surface stress [21–24]. While cantilevers with lower spring constants are indeed more sensitive to an applied surface stress, this approach also amplifies the parasitic deflections arising from non-specific interactions. Another strategy is to perform measurements in differential mode, where the response of a second 'passivated' reference cantilever is subtracted from the main surface stress signal in an attempt to eliminate parasitic effects (due to vibration, temperature changes, non-specific binding, etc) which affect sensor performance. Nevertheless, this approach can fail if the origin of the chemical/physical signal is poorly understood, as the reference cantilever can be rendered completely inert to any chemical stimuli and thus cannot subtract parasitic non-specific chemical interactions. To date, several papers have described the use of cantilever-based surface stress sensing for biomolecular detection. While the breadth of potential applications is impressive, the sensor response is often near the minimum detectable level of this technology, with induced surface stresses ranging from 0.001 to 0.05 N m^{-1} [11–15].

Despite the increasing number of demonstrated applications, surprisingly few studies have explored the physical origins of the induced surface stress involved in specific sensing applications [25–29]. Evidently, surface stress generation during molecular adsorption can involve several types of interactions which can all contribute to the overall mechanical response of the cantilever. Intermolecular, interactions (van der Waals and Pauli exclusion) described by the Lennard-Jones potential, as well as electrostatic forces between adsorbates have previously been proposed as mechanisms for the origins of the observed surface stresses [2, 11, 30–32]. Another mechanism [33–37], which is often neglected in (bio)-molecular sensing applications, involves the disruption of the electronic charge distribution of the substrate's surface atoms, due to direct interaction between adsorbates and surfaces.

In this paper, we explore various mechanisms associated with molecular adsorption on the cantilever's surface and their impact on induced surface stresses. We also propose that, armed with a fundamental understanding of the dominant sources of surface stress, one can optimize and propose innovative sensing strategies that are designed to maximize the induced surface stress signal. We estimate that improvements of one or two orders of magnitude over typical published results should be possible. In combination with reduction of cantilever noise by well understood scaling of its dimensions [24, 38], addressing systems design issues [39–41] and using differential measurements techniques, the fundamental concepts presented herein should make the cantilever-based sensor a more reliable and competitive approach to sensing.

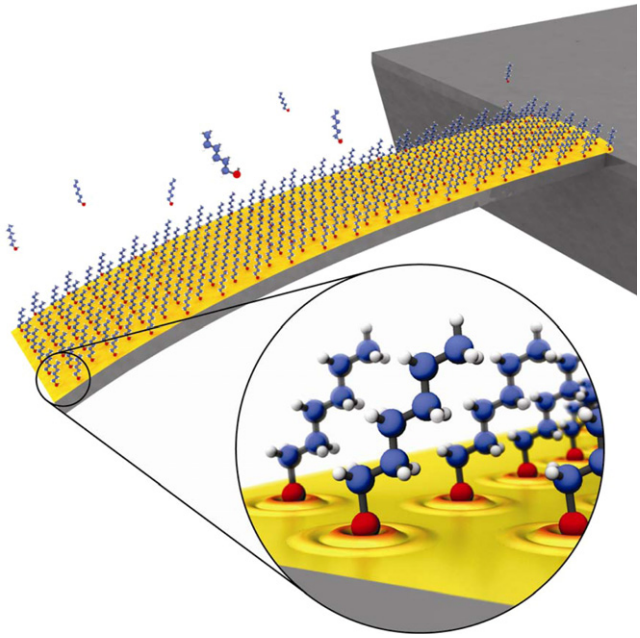

Figure 1. Artistic view of an alkanethiol self-assembled monolayer (SAM) on a gold-coated microcantilever formed from the gas phase. Various interactions can contribute to the overall observed surface stress during molecular adsorption onto surfaces, such as Lennard-Jones interactions, Coulombic repulsion between adsorbed molecules or adsorption-induced changes in the electronic charge density at the metal's surface. Inset: close-up view of hexanethiol (C6) molecules adsorbed on a gold surface, highlighting the redistribution of the electronic structure of the gold surface due to the creation of the $Au^{+}S^{-}$ bond and the associated electronic charge transfer from the gold to the thiol molecule.

The adsorption of alkanethiol molecules (and the formation of self-assembled monolayers) on gold-coated cantilevers has been investigated as a model system to elucidate the origins of the surface stress (figure 1). Several microscopic mechanisms for the source of the observed surface stress are considered, and first-order models are compared to experimental results.

2. Experimental results

The surface stress induced during the formation of alkanethiol SAMs from the gas phase was measured as a function of molecular chain length. A custom cantilever-based sensor was used to measure the surface stress induced by SAM formation from the gas phase on gold-coated cantilevers [42]. In these experiments, the Au(111) surfaces were prepared by thermal evaporation under identical deposition conditions (see supporting information section available at stacks.iop.org/Nano/21/075501/mmedia). As a result, the gold surface morphology was similar for all experiments, exhibiting a grain size of 500 ± 400 nm as assessed by scanning tunneling microscopy. Figure 2 shows a graph of the mean steady-state surface stress induced by the formation of hexanethiol (C6), octanethiol (C8), and decanethiol (C10) SAMs on gold-coated cantilevers. The

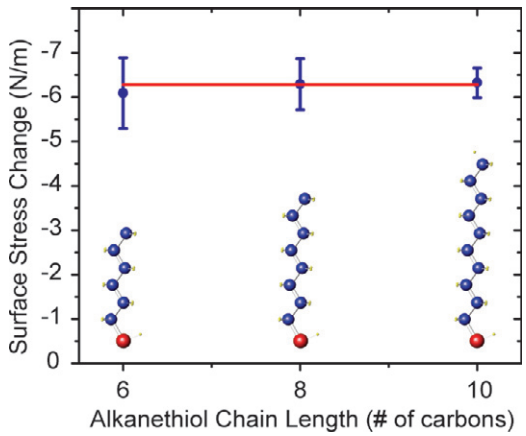

Figure 2. The mean steady-state surface stress resulting from hexanethiol (C6), octanethiol (C8) and decanethiol (C10) SAM formation on gold-coated cantilevers. A chain length independent compressive change in surface stress of -6.3 ± 0.2 N m^{-1} was measured at equilibrium coverage. The gold substrates used in these experiments had grain sizes of 500 ± 400 nm. The error bars are the standard errors associated with the number of experiments performed for each chain length (3 for C6, 4 for C8 and 11 for C10).

steady-state surface stress is taken as that when a constant surface stress value has been attained for several minutes of time. The data obtained demonstrate that the induced surface stress is independent of molecular chain length for this range of molecules. A total of 18 measurements are included in figure 2, which show a constant overall mean compressive change in surface stress of -6.3 ± 0.2 N m^{-1}.

Scanning tunneling microscopy (STM) was used to assess the alkanethiol SAMs formed under these conditions. As highlighted in our previous work [43], we confirmed that these monolayers are of high quality and primarily in the 'standing-up' phase.

Our finding that surface stress is independent of alkanethiol chain length conflicts with the results of Berger *et al* [2] where a chain length dependence was observed. However, that report did not specify the Au substrate grain size nor did it try to assess the quality of the monolayers. Based on the magnitude of the reported surface stress in [2], it is most probable that their resulting alkanethiol SAMs were incompletely formed (not in the standing-up phase) and were likely kinetically trapped in an intermediate lying-down phase. This conclusion is based on our previous work [43] which shows that alkanethiol SAMs formed from the vapor phase on Au surfaces with grain sizes smaller than 90 nm remain kinetically trapped in a lying-down phase, in contrast to SAMs formed on large Au grains where STM imaging shows a predominance of the expected standing-up phase. The average gold surface grain size has been found to have a significant impact on the integrity of the resulting SAM and consequently on the induced surface stress. For example, a 25-fold change in surface stress has been observed with increasing grain size [44]. Recent studies [45, 46] confirm this dependency of the SAM structure on induced surface stress for alkanethiols of different lengths.

The results presented in figure 2 (chain length *independence*) suggest that the interactions between adjacent alkyl chains (of different lengths; C6, C8, or C10) do not play a significant role in generating the observed large surface stress. Any model that seeks to explain the origin of the surface stress should consider the lack of chain length dependence.

3. Modeling results: microscopic origins of surface stress

The adsorption of target molecules onto a surface is governed by several physical/chemical interactions, all of which can potentially contribute to measurable surface stresses. Here, we consider three different interactions and their contributions to the overall observed surface stress. Firstly, Lennard-Jones interactions between adsorbed molecules can be attractive (van der Waals) or repulsive (Pauli exclusion), resulting in a surface stress. Secondly, electrostatic interactions between adjacent Au–thiol bonds may also lead to a measurable surface stress. Finally, redistribution of the electronic structure of the substrate surface atoms due to the adsorption of the target molecules will modify the surface's local free energy, and will result in a change in surface stress. Note that a discussion of swelling and hydration of specific or unspecific sensing layers [25, 47, 48] on cantilevers is beyond the scope of this paper, as the alkanethiol model system investigated here does not show these additional complexities. These interactions often involve complex sensing structures (such as grafted polymers or ssDNA probes) and dynamic mixtures of analytes (ionic exchange with the sensing layer) [25, 31, 47–49]. Simple modeling was undertaken with respect to the gas phase adsorption of alkanethiol molecules onto a gold surface to determine the contribution of these various interactions to the overall observed surface stress [50].

3.1. Lennard-Jones interactions

Lennard-Jones interactions between molecules adsorbed on a surface can produce a measurable surface stress [27] in certain systems. However, we find that such interactions do not account for the large compressive surface stresses measured for the formation of alkanethiol SAMs on gold surfaces. Energy minimization calculations (see supporting information section available at stacks.iop.org/Nano/21/075501/mmedia) using the Universal Force Field approach [51] reveal optimized intermolecular separations of 0.47 nm and 0.44 nm between two parallel decanethiol and decane molecules, respectively. This suggests that a surface stress resulting from such interactions would be tensile (attractive), since these are smaller than the 0.50 nm intermolecular separation of alkanethiols in a SAM formed on an Au(111) surface, given the $(\sqrt{3} \times \sqrt{3})$R30° structure of the standing-up phase[9]. As illustrated in figure 3(A), these interactions described by the Lennard-Jones potential lead to the familiar tilt angle (to reduce intermolecular distances) of the alkyl chains present in the SAM [52]. The experimentally measured surface stresses induced by alkanethiol SAM formation are compressive.

[9] $\sqrt{3} \times 0.288\,37$ nm $\approx 0.499\,47$, 0.288 37 nm being the closest interatomic spacing of bulk gold.

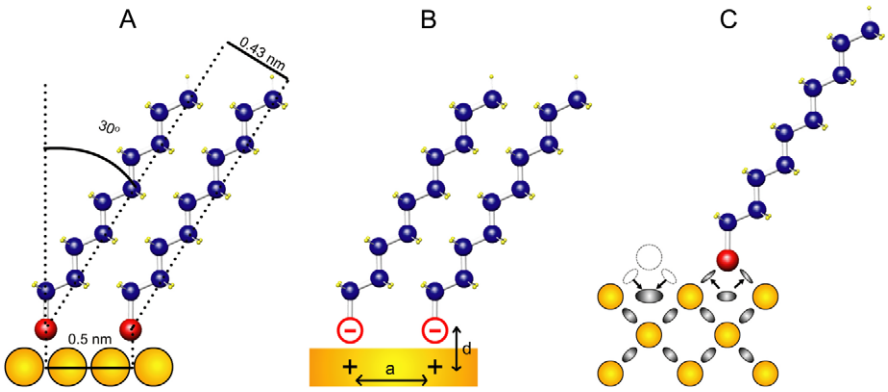

Figure 3. Alkanethiol molecules adsorbed onto gold surfaces. Lennard-Jones interactions (A) between adjacent alkanethiol molecules result in a molecular tilt to reduce inter-chain distances. Electrostatic repulsion (B) between adjacent Au^+S^- bonds generates a compressive surface stress. In a SAM, these charges appear as two 'sheets' of point charges separated by a distance, d. The intermolecule distance, a, is the distance between adjacent thiol (sulfur) headgroups. Alkanethiol adsorption onto a gold surface modifies the electronic charge distribution near the gold surface (C), altering the local electron density and resulting in changes in surface stress.

Surface pressure measurements performed using the Langmuir–Blodgett technique for alkanethiols on a liquid surface, which provide a measure of the repulsive component of the intermolecular interactions described by the Lennard-Jones potential, are consistent with the above analysis. Since molecules are not anchored to a solid surface, these surface pressure measurements provide an estimate for the compressive surface stress resulting almost exclusively from intermolecular interactions as a function of molecular area (area per unit cell). In a recent study, Broniatowski [53] confirms that repulsive interactions (i.e. compressive change in surface stress) at room temperature are negligible for molecular areas typically found in highly ordered alkanethiol SAMs on Au(111) (0.22 nm^2/molecule for the ($\sqrt{3} \times \sqrt{3}$)R30° structure). At higher packing densities, surface pressure increases to approximately 10–15 mN m^{-1} before the monolayer collapses at molecular areas of about 0.125 nm^2. To generalize, we expect surface stresses resulting purely from Lennard-Jones-type interactions at typical packing densities to be on the order of $\pm$0.001–0.01 N m^{-1}.

3.2. Electrostatic interactions

Electrostatic repulsion between the adsorbed molecules has been proposed as a possible source of the observed surface stress [2] for the alkanethiol SAM system. In fact, the Au–S bond is slightly polar, as it is accompanied by a shift in electron density from the Au towards the S atom resulting in a Au^+S^- bond [54–57]. When a complete SAM is formed on a gold surface, a series of adjacent dipoles are pinned to the surface, all repelling each other through Coulombic interactions, as depicted in figure 3(B).

The electrostatic energy contribution to the surface stress can be evaluated in a rather simplistic model where the electrostatic energy is summed over all Au^+S^- bonds. This total electrostatic energy, $\boldsymbol{E}_{\mathrm{es-tot}}$, is counterbalanced by a restoring elastic energy, $\boldsymbol{E}_{\mathrm{cantilever}}$, resulting from the bent surface of the cantilever. Minimization of the sum of these two energy contributions yields an equilibrium intermolecular separation, which can be converted and interpreted as a surface stress (see supporting information section available at stacks.iop.org/Nano/21/075501/mmedia).

Calculations using typical dipole charges and lengths show that the induced surface stress is much smaller than that experimentally measured. A compressive surface stress of -0.10 N m^{-1} arises when an alkanethiol SAM forms on a gold surface given an expected charge transfer of $0.2e$ [54] and a charge separation of 0.2 nm [58, 59] (see supporting information section available at stacks.iop.org/Nano/21/075501/mmedia). Even if one assumes that some charge travels up the alkyl chain, effectively increasing the dipole length, electrostatic interactions only account for at most 10% of the large compressive surface stresses measured experimentally.

3.3. Charge transfer and surface charge redistribution

Changes in the electronic charge density at the gold surface can account for the generation of large surface stresses. To illustrate this concept, consider the effect of cleavage of noble metal surfaces on the surface stress. A tensile surface stress results when a clean metal surface is created since the electronic charge density surrounding surface atoms is different than that surrounding bulk atoms. As depicted in figure 3(C), the loss of bonds at the newly formed surface triggers an electronic redistribution which causes an increased charge density between the top surface atoms, often observed as a tensile surface stress resulting from the increase in the attractive interaction (bond strength) between surface atoms [35]. In the case of gold, this tensile surface stress is large enough to initiate the Au(23 × 3) surface reconstruction [33]. In the same way, when an adsorbate binds to a clean metal surface, the charge density at the surface is again disrupted, and, for electronegative adsorbates, is usually accompanied by a reduction of the tensile surface stress, i.e. a compressive change in surface stress [35]. In some instances, these changes in surface stress can be exceptionally large, as in the case [60] of the gas

phase adsorption of Ag on a Pt(111) surface (-5.9 N m^{-1} per adsorbed monolayer, with as much as -20 N m^{-1} for seven monolayers). Important changes in surface stress are also observed in electrochemically-controlled deposition of metals and adsorption of ions in electrolyte solutions [61–63]. It was highlighted by Ibach that in such cases of direct interactions between adsorbates and metal surfaces, the induced compressive surface stress is mainly caused by changes in the charge distribution near the surface of the metal substrate, and that the direct repulsive interactions between adsorbates (including dipolar interactions) contribute little to the overall surface stress [64]. For example, a complete Bi monolayer electrochemically deposited on Au(111) causes an overall surface stress change of about -1.4 N m^{-1} via changes in the electronic state of the underlying metal substrate [65]. Similarly, the electrochemically-driven adsorption of ions on metal electrodes can produce surface stresses on the order of -1 N m^{-1} [44, 63, 66].

It is clear that the atomistic details of the underlying electronic charge redistribution vary from system to system, but that relatively large adsorption-induced surface stresses can be induced. The magnitude and anisotropy of the induced surface stress can be affected by several factors including the details of the electronic structure at the metal surface, the strength of the adsorbate–metal interaction (e.g., covalent, ionic bonds), surface modification and relaxation effects (e.g., surface reconstruction, creation of atomic vacancies/etching, etc), adsorption-induced changes in substrate elastic properties, and the relative strength of competing adsorbates. This last aspect involves an exchange interaction at the interface whereby the adsorption of targets will displace either weakly bound gas or water molecules (typically at the gas–solid interface), or moderately bound ionic species (typically at the liquid–solid interface). The relative strengths of interactions involved during this exchange influences the net measurable change in surface stress. We postulate that this can account for the large surface stress induced upon alkanethiol SAM formation on Au(111) from the gas phase relative to measurements (on various systems) performed in liquid (where weakly bound ionic or polar species are displaced). Some research has been focused on exploring these intricacies [29, 33, 35, 36, 63, 66–69]. These add some complexities in interpreting results. We will not expand on the details of these mechanisms here. Instead, we focus on the magnitude of the surface stresses resulting from these types of interactions in general, which contribute significantly to the generation of surface stress compared to other sources such as inter-adsorbate Lennard-Jones or Coulombic interactions.

Alkanethiol adsorption onto a gold surface redistributes the electronic structure of the gold surface due to the creation of the Au^+S^- bond and the associated electronic charge transfer from the gold to the thiol molecule, as depicted in figure 3(C). This effectively reduces the bond strengths between Au surface atoms, increases interatomic distances (decreasing the density of gold surface atoms), and thus generates a compressive change in surface stress. This effect can result in large surface stresses and is consistent with the experimentally measured compressive surface stresses of -6.3 ± 0.2 N m^{-1} (figure 2). In fact, these large compressive changes in surface stresses have been shown to modify the Au(23×3) reconstruction [70–72] of the gold surface. We suggest that the large surface stress induced by alkanethiol adsorption provides the necessary driving force for the ejection of Au surface atoms that subsequently diffuse and form etch pits or vacancy islands, which is known to accompany alkanethiol SAM formation [72]. Moreover, since the electronic charge distribution at the gold surface is identical for adsorbed alkanethiol molecules containing more than three carbon atoms [73], this mechanism for the generation of surface stress is in fact consistent with our observation that the induced surface is chain length independent for hexanethiol, octanethiol and decanethiol.

The above discussion of the three different sensing mechanisms provides order of magnitude estimates for their associated expected surface stress. The experimental and modeling results presented herein allow us to conclude that, generally, interactions described by the Lennard-Jones potential can yield small compressive surface stresses of 0.001–0.01 N m^{-1}, whereas Coulombic interactions (derived from the repulsion of adjacent Au^+S^- dipoles) are intermediate in magnitude and typically generate around 0.01–0.1 N m^{-1}, both depending on packing densities and in the latter case, the amount of charge involved. To increase the signal strength in a specific application, interactions that will generate maximum surface stress response ought to be favored. Surface stress as large as 1–10 N m^{-1} can be expected if adsorption and/or chemical recognition by the sensing layer, in the absence of competing adsorbates, lead to changes in the charge density of the underlying metal substrate.

4. Discussion: sensing applications

While there are several examples in the literature related to using cantilever-based sensing for the detection of various biomolecules, all of them involve relatively small induced surface stresses (0.001–0.05 N m^{-1}), implying that adsorption-induced changes in the electronic structure of the underlying metal surface is not the dominant mechanism in these experiments. In these cases, as suggested in the literature, the measured change in surface stress most often originates from Lennard-Jones or weak electrostatic intermolecular interactions. However, potential weak changes in electronic structure of the underlying metal surface moderated through an insulating receptive molecular layer cannot be entirely ruled out as a possible parallel mechanism. Generally, such receptive layers shield or 'protect' the underlying metal surface from adsorbed targets. Nevertheless, the presence of slight defects or pinholes in the receptive layer, or an adsorption-induced reorganization of the receptive layer or electric double layer, might translate into weak but non-negligible changes in the electronic density of the metal surface (observed as an induced surface stress).

Armed with an understanding of the types of interactions that can generate the most amount of surface stress, it is possible to optimize the response of cantilever-based sensors by suitably tailoring the chemical properties of the sensing

and transduction layer [50, 74]. In so doing, one needs to favor target–cantilever interactions that promote changes in the electronic structure of the metal surface, as opposed to relying on either intermolecular Lennard-Jones or Coulombic interactions. One approach would be to immobilize an incomplete (sub-monolayer) but protective receptive layer on the metal substrate, upon which the recognition of the molecular targets exposes regions of the metal (e.g. due to conformation changes of the receptive layer probes). Subsequently, secondary molecules that interact directly with the newly exposed metal surface can be used as surface stress enhancers. In other words, while the primary target-receptor recognition event might generate small surface stresses, the secondary 'surface stress enhancers', initially prevented from interacting with the underlying metal substrate, will interact with the newly-revealed surface sites and modify the electronic structure of the metal surface to generate much larger surface stresses. Alternatively, another more controlled approach, following Rant *et al* [75], would be to dynamically switch the structural conformation of the molecules on the metal substrate by an electric field to reveal surface sites to the electrolyte. Detection of a specific target would be based on the difference in the induced surface stress upon molecular recognition by the probe layer.

In order to illustrate the validity of these approaches, we turn to electrochemistry. Measurements were performed using a microcantilever-based sensor where the cantilever is also the working electrode (WE) in a standard three-probe electrochemical system, the details of which are described elsewhere [76]. This system allows for the measurement of surface stress that occurs during the electrochemically-controlled adsorption/desorption of adsorbates onto/from the cantilever's gold-coated surface. As such, this allows us to quantify the surface stress associated with potential-induced anion adsorption on bare Au and alkanethiol SAM modified surfaces.

Figure 4 shows the surface stress change as a function of potential in 100 mM NaCl for (figure 4(a)) a dodecanethiol SAM modified electrode, (figure 4(b)) a defective SAM (less than 100% coverage; sub-monolayer) and (figure 4(d)) a clean bare Au surface. To illustrate the effect of both weak and strong adsorption, the surface stress on a bare Au surface induced by ClO_4^- (figure 4(c)) and Cl^- (figure 4(d)) were also compared. As the potential is increased, the adsorption of anions takes place to compensate for the positive charging of the microcantilever surface (deficit of electrons), which results in a compressive change in surface stress as expected based on the simple bonding model described above. The difference between two anion species illustrates the fact that, for a given potential change, the change in charge density in the metal, at a particular electrolyte concentration, dictates the capacitance of the metal/solution interface and the induced surface stress [44]. Although more potential-induced surface stress is observed for the case of Cl^-, the change in surface stress for a given change in surface charge density for an Au(111) surface is in fact greater for weaker adsorbing ClO_4^- anions as demonstrated by Haiss [63], since significantly less charge is transferred at the interface and remains at the metal surface. This has also been demonstrated on microcantilever surfaces [44], showing quantitative agreement with *ab initio* studies of surface stress response to charging [68].

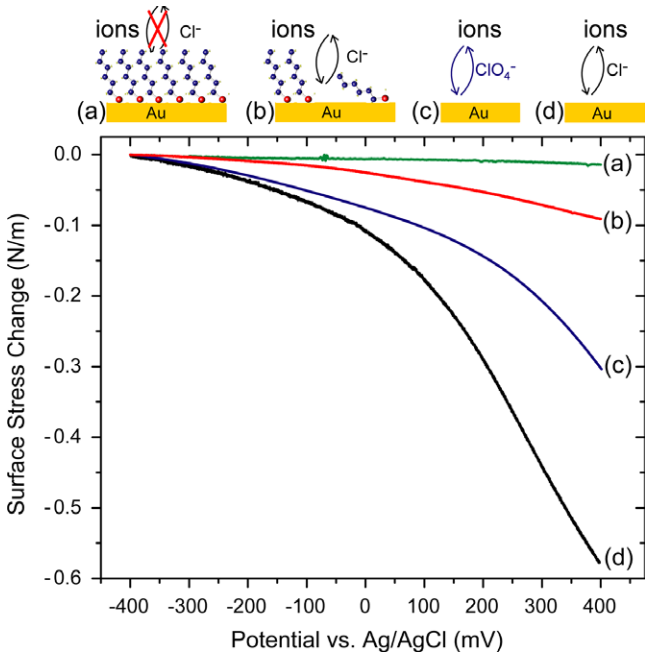

Figure 4. Change in the surface stress as a function of electrode potential in 100 mM NaCl of (a) a SAM modified Au-coated cantilever, (b) defective SAM, (c) bare Au in 100 mM $HClO_4$ and (d) bare Au in 100 mM NaCl. The change in surface stress values were arbitrarily set to zero at the most negative potential.

When the surface is covered ('protected') by a fully formed alkanethiol SAM (figure 4(a)) the surface stress induced by the interaction of anions with the surface is severely reduced. Over the potential window investigated the surface stress varied by less than 0.01 N m^{-1}. As expected, the potential-induced surface stress is amplified with increasing number of defects in the SAM as shown by figure 4(b) (SAM defect density was quantified by monitoring the magnitude of the leakage current). The electrochemically-controlled adsorption of anions at the defect sites (unoccupied Au binding sites) can thus generate a surface stress response of approximately -0.1 N m^{-1} or larger if more and/or stronger ions are allowed to adsorb. These results provide experimental evidence to support the proposed mechanism of surface stress enhancement during biomolecular recognition.

5. Conclusions

Various interactions drive molecular adsorption onto surfaces, all of which can result in measurable surface stresses. While, in most cantilever-based sensing applications, interactions described by the Lennard-Jones potential and Coulombic repulsion between adsorbed molecules generate relatively small surface stresses, adsorption-induced changes in the electronic charge density at the metal's surface can result in much larger surface stresses. In the case of the direct adsorption of alkanethiol molecules on gold surfaces, we

measured a chain length independent surface stress of -6.3 ± 0.2 N m^{-1}, consistent with this latter interaction.

Current cantilever-based sensing applications can significantly gain in performance by taking these findings into account. Modifying the sensing architecture such that molecular adsorption inherently modifies the charge density of the underlying metal surface will result in the generation of much larger surface stresses and greatly improved sensor performance. At the moment, the commonly used thiol linkage is mainly structural and lacks an essential orbital conduit for electrons and/or holes to influence the underlying gold electronic structure upon recognition. Ideally, the receptive layer should be designed to trigger charge transfer reactions only for specific biomolecular recognition events.

Acknowledgments

This work was supported by the Natural Science and Engineering Research Council of Canada (NSERC) and Canadian Institutes of Health Research (CIHR). MG and VT-C acknowledge the financial support given by McGill University through its McGill Major Fellowships program, Le Fonds Québécois de la Recherche sur la Nature et les Technologies (FQRNT), and the Natural Sciences and Engineering Council of Canada (NSERC). The authors thank H Bourque and I J Burgess for helpful discussions, E Del Campo for machining the instrument, R Gagnon for technical assistance and James Hedberg for his artistic input.

References

[1] Gimzewski J K, Gerber Ch, Meyer E and Schlittler R R 1994 *Chem. Phys. Lett.* **217** 589–94
[2] Berger R, Delamarche E, Lang H P, Gerber Ch, Gimzewski J K, Meyer E and Güntherodt H-J 1997 *Science* **276** 2021–4
[3] Berger R, Gerber Ch and Gimzewski J K 1996 *Anal. Methods Instrum.* 74–7 (special issue μTAS'96)
[4] Ilic B, Craighead H G, Krylov S, Senaratne W, Ober C and Neuzil P 2004 *J. Appl. Phys.* **95** 3694–703
[5] Nugaeva N, Gfeller K Y, Backmann N, Lang H P, Düggelin M and Hegner M 2005 *Biosens. Bioelectron.* **21** 849–56
[6] Barnes J R, Stephenson R J, Welland M E, Gerber Ch and Gimzewski J K 1994 *Nature* **372** 79–81
[7] Thundat T, Sharp S L, Fischer W G, Warmack R J and Wachter E A 1995 *Appl. Phys. Lett.* **66** 1563–5
[8] Varesi J, Lai J, Shi Z, Perazzo T and Majumdar A 1997 *Appl. Phys. Lett.* **71** 306–8
[9] Manalis S R, Minne S C, Quate C F, Yaralioglu G G and Atalar A 1997 *Appl. Phys. Lett.* **70** 3311–3
[10] Fritz J 2008 *Analyst* **133** 855–63
[11] Fritz J, Baller M K, Lang H P, Rothuizen H, Vettiger P, Meyer E, Güntherodt H-J, Gerber Ch and Gimzewski J K 2000 *Science* **288** 316–8
[12] McKendry R *et al* 2002 *Proc. Natl Acad. Sci. USA* **99** 9783–8
[13] Zhang J, Lang H P, Huber F, Bietsch A, Grange W, Certa U, McKendry R, Güntherodt H-J, Hegner M and Gerber Ch 2006 *Nat. Nanotechnol.* **1** 214–20
[14] Wu G, Datar R H, Hansen K M, Thundat T, Cote R J and Majumdar A 2001 *Nat. Biotechnol.* **19** 856–60
[15] Savran C A, Knudsen S M, Ellington A D and Manalis S R 2004 *Anal. Chem.* **76** 3194–8
[16] Berger R, Gerber C, Lang H P and Gimzewski J K 1997 *Microelectron. Eng.* **35** 373
[17] Baller M K *et al* 2000 *Ultramicroscopy* **82** 1
[18] Pinnaduwage L A *et al* 2003 *Nature* **425** 474
[19] Li P, Li X, Zuo G, Liu J, Wang Y, Liu M and Jin D 2006 *Appl. Phys. Lett.* **89** 074104
[20] Thundat T, Wachter E A, Sharp S L and Warmack R J 1995 *Appl. Phys. Lett.* **66** 1695–7
[21] Ransley J H T, Watari M, Sukumaran D, McKendry R A and Seshia A A 2006 *Microelectron. Eng.* **83** 1621–5
[22] Thaysen J, Yalçinkaya A D, Vettiger P and Menon A 2002 *J. Phys. D: Appl. Phys.* **35** 2698–703
[23] Yu X, Thaysen J, Hansen O and Boisen A 2002 *J. Appl. Phys.* **92** 6296–301
[24] Li M, Tang H X and Roukes M L 2007 *Nat. Nanotechnol.* **2** 114–20
[25] Hagan M F, Majumdar A and Chakraborty A K 2002 *J. Phys. Chem.* B **106** 10163–73
[26] Liu F, Zhang Y and Ou-Yang Z-C 2003 *Biosens. Bioelectron.* **18** 655–60
[27] Dareing D W and Thundat T 2005 *J. Appl. Phys.* **97** 043526
[28] Zhang J-Q, Yu S-W, Feng X-Q and Wang G-F 2008 *J. Appl. Phys.* **103** 093506
[29] Sushko M L, Harding J H, Shluger A L, McKendry R A and Watari M 2008 *Adv. Mater.* **20** 3848–53
[30] Wu G-H, Ji H-F, Hansen K, Thundat T, Datar R, Cote R, Hagan M F, Chakrabory A K and Majumdar A 2001 *Proc. Natl Acad. Sci. USA* **98** 1560–4
[31] Stachowiak J C, Yue M, Castelino K, Chakraborty A and Majumdar A 2006 *Langmuir* **22** 263–8
[32] Watari M, Galbraith J, Lang H-P, Sousa M, Hegner M, Gerber Ch, Horton M A and McKendry R A 2007 *J. Am. Chem. Soc.* **129** 601–9
[33] Haiss W 2001 *Rep. Prog. Phys.* **64** 591
[34] Sander D 2003 *Curr. Opin. Solid State Mater. Sci.* **7** 51–7
[35] Ibach H 1997 *Surf. Sci. Rep.* **29** 193–64
[36] Feibelman P J 1997 *Phys. Rev.* B **56** 2175–82
[37] Varadharajan S, Giancarlo C and Grossman J C 2008 *Phys. Rev. Lett.* **101** 185504
[38] Lavrik N V, Sepaniak M J and Datskos P G 2004 *Rev. Sci. Instrum.* **75** 2229
[39] Sheehan P E and Whitman L J 2005 *Nano Lett.* **5** 803–7
[40] Naira P R and Alam M A 2006 *Appl. Phys. Lett.* **88** 233120
[41] Squires T M, Messinger R J and Manalis S R 2008 *Nat. Biotechnol.* **26** 417
[42] Godin M, Laroche O, Tabard-Cossa V, Beaulieu L Y, Williams P J and Grutter P 2003 *Rev. Sci. Instrum.* **74** 4902–7
[43] Godin M, Williams P J, Tabard-Cossa V, Laroche O, Beaulieu L Y, Lennox R B and Grutter P 2004 *Langmuir* **20** 7090–6
[44] Tabard-Cossa V, Godin M, Burgess I, Monga T, Lennox R B and Grutter P 2007 *Anal. Chem.* **79** 8136–43
[45] Desikan R, Armel S, Meyer H M III and Thundat T 2007 *Nanotechnology* **18** 424028
[46] Kohale S, Molina S M, Weeks B L, Khare R and Hope-Weeks L J 2007 *Langmuir* **23** 1258–63
[47] Mertens J, Rogero C, Calleja M, Ramos D, Martin-Gago J A, Briones C and Tamayo J 2008 *Nat. Nanotechnol.* **3** 301–7
[48] Tabard-Cossa V, Godin M, Burgess I, Lennox R B and Grutter P 2005 *J. Phys. Chem.* B **109** 17531–7
[49] Lang H P, Baller M K, Berger R, Gerber Ch, Gimzewski J K, Battiston F M, Fornaro P, Ramseyer J P, Meyer E and Güntherodt H J 1999 *Anal. Chim. Acta* **393** 59–65
[50] Godin M 2004 *PhD Thesis* McGill University Montréal, Canada
[51] Rappé A K, Casewit C J, Colwell K S, Goddard W A III and Skiff W M 1992 *J. Am. Chem. Soc.* **114** 10024

[52] Ulman A, Eilers J E and Tillman N 1989 *Langmuir* **5** 1147–52
[53] Broniatowski M 2009 *J. Colloid Interface Sci.* **337** 183–90
[54] Bourg M-C, Badia A and Lennox R B 2001 *J. Phys. Chem.* B **104** 6562
[55] Hayashi T, Morikawa Y and Nozoye H 2001 *J. Chem. Phys.* **114** 7615
[56] Poirier G E, Fitts W P and White J M 2001 *Langmuir* **17** 1176
[57] Groenbeck H, Curioni A and Andreoni W 2000 *J. Am. Chem. Soc.* **122** 3839
[58] Yourdshahyan Y and Rappe A M 2002 *J. Chem. Phys.* **117** 825
[59] Kaun C-C and Guo H 2003 *Nano Lett.* **3** 1521
[60] Grossmann A, Erley W, Hannon J B and Ibach H 1996 *Phys. Rev. Lett.* **77** 127
[61] Friesen C, Dimitrov N, Cammarata R C and Sieradzki K 2001 *Langmuir* **17** 807
[62] Seo M and Yamazaki M 2004 *J. Electrochem. Soc.* **151** E276
[63] Haiss W, Nichols R J, Sass J K and Charle K P 1998 *J. Electroanal. Chem.* **452** 199–202
[64] Ibach H 1999 *Electrochim. Acta* **45** 575–81
[65] Stafford G R and Bertocci U 2006 *J. Phys. Chem.* B **110** 15493
[66] Viswanath R N, Kramer D and Weissmüller J 2008 *Electrochim. Acta* **53** 2757–67
[67] Nichols R J, Nouar T, Lucas C A, Haiss W and Hofer W A 2002 *Surf. Sci.* **513** 263–71
[68] Umeno Y, Elsasser C, Meyer B, Gumbsch P, Nothacker M, Weissmuller J and Evers F 2007 *Europhys. Lett.* **78** 13001
[69] Weigend F, Evers F and Weissmuller J 2006 *Small* **2** 1497
[70] Dishner M H, Hemminger J C and Feher F J 1997 *Langmuir* **13** 2318
[71] Fitts W P, White J M and Poirier G E 2002 *Langmuir* **18** 1561
[72] Poirier G E 1997 *Langmuir* **13** 2019
[73] Kaun C-C and Guo H 2004 Based on *ab inition* calculation, private communication
[74] Tabard-Cossa V 2005 *PhD Thesis* McGill University Montréal, Canada
[75] Rant U, Arinaga K, Fujita S, Yokoyama N, Abstreiter G and Tornow M 2004 *Nano Lett.* **4** 2441–5
[76] Tabard-Cossa V, Godin M, Beaulieu L Y and Grutter P 2005 *Sensors Actuators* B **107** 233–41